Published in final edited form as:
Heart Rhythm. 2014 November ; 11(11): 2064–2072. doi:10.1016/j.hrthm.2014.07.022.

CELLULAR MECHANISM OF PREMATURE VENTRICULAR CONTRACTION-INDUCED CARDIOMYOPATHY

Youhong Wang, PhD[1], **Jose M. Eltit, PhD**[1], **Karoly Kaszala, MD, PhD, FHRS**[1,2], **Alex Tan, MD**[1,2], **Min Jiang, PhD**[1], **Mei Zhang, PhD**[1], **Gea-Ny Tseng, PhD, FAHA**[1], and **Jose F. Huizar, MD, FHRS**[1,2,3]

[1]Department of Physiology & Biophysics, Virginia Commonwealth University

[2]McGuire VA Medical Center

[3]Pauley Heart Center of Virginia Commonwealth University, Richmond, Virginia

Abstract

Background—Frequent premature ventricular contractions (PVCs) are associated with increased risk for sudden cardiac death (SCD) and can cause secondary cardiomyopathy (CM).

Objective—We sought to determine the mechanism(s) responsible for prolonged refractory period and LV dysfunction demonstrated in our canine model of PVC-induced CM.

Methods—Single myocytes were isolated from LV free wall of PVC and control canines, and used for patch clamp recording, $[Ca]_i$ measurements and immunocytochemistry/confocal microscopy. LV tissues adjacent to area of myocyte isolation were used for immunoblot quantification of protein expression.

Results—In PVC group, LVEF declined from 57.6±1.5% to 30.4±3.1% after ≥ 4 months of ventricular bigeminy. Compared to control myocytes, PVC myocytes had reduced densities of both outward (I_{to} and I_{K1}) and inward (I_{CaL}) currents, but no consistent changes in I_{Kr} or I_{Ks}. The reduction in I_{to}, I_{K1} and I_{CaL} was accompanied by decreased protein levels of their channel subunits. The degrees of reduction in I_{to}, I_{K1} and I_{CaL} varied among PVC myocytes, creating marked heterogeneity in action potential (AP) configurations and durations. PVC myocytes showed impaired Ca-induced Ca release from SR, without increase in SR Ca leak or decrease in SR Ca store. This was accompanied by a decrease in dyad scaffolding protein, junctophilin-2, and loss of Cav1.2 registry with Ca-releasing channels (RyR2).

Conclusion—PVCs increase dispersion of AP configuration/duration, a risk factor for SCD, due to heterogeneous reduction in I_{to}, I_{K1} and I_{CaL}. The E-C coupling is impaired due to decrease in I_{CaL} and Cav1.2 misalignment with respect to RyR2.

Keywords

Premature ventricular contraction; cardiomyopathy; electrical remodeling; excitation-contraction coupling

For correspondence: Gea-Ny Tseng, PhD, Department of Physiology & Biophysics, Virginia Commonwealth University, 1101 E. Marshall Street, Richmond, VA 23298, Phone: 804-827-0811, Fax: 804-828-7382, gtseng@vcu.edu.

INTRODUCTION

Frequent premature ventricular contractions (PVCs) have been associated with an increased risk of sudden cardiac death (SCD) and identified as a possible cause of non-ischemic cardiomyopathy (CM). Our canine model of PVC has shown that chronic exposure (12 weeks) of frequent PVCs (ventricular bigeminy, 240 ms coupling interval) impaired ventricular contractile function[1]. These observations established frequent PVC as an entity causing cardiomyopathy (PVC-induced cardiomyopathy). Surprisingly, despite LV contractile dysfunction, there were no detectable structural abnormalities[1]. Therefore, PVC-induced cardiomyopathy appears to be a functional abnormality. Consistent with these findings, LVEF recovered toward normal within 2 to 4 weeks after discontinuation of PVCs[1].

The mechanism for PVC-induced cardiomyopathy is not clear. Furthermore, it is uncertain whether or how chronic PVCs may induce electrical remodeling, that may contribute to the increased risk for sudden cardiac death (SCD) observed in some patients with frequent PVCs. The current study was designed to address these issues using four complementary approaches. First, patch clamp recordings of single LV myocytes were used to study how chronic PVCs affected action potentials and key ionic currents shaping the action potentials. Second, immunoblots of whole tissue lysates were used to quantify the expression levels of proteins of interest. Third, monitoring of intracellular [Ca] in LV myocytes was used to evaluate whether chronic PVCs affected Ca_i handling. Fourth, immunocytochemistry in conjunction with confocal microscopy was used to assess the organization of t-tubules and junctional SR (dyads) and proteins involved in excitation-contraction (E-C) coupling.

METHODS

Animal model

Under general anesthesia, 5 mongrel dogs (> 10 months old; weight, 35 to 45 lbs) underwent implantation of an experimental pacemaker through left thoracotomy. After recovery for 2–3 weeks, ventricular bigeminy (50% PVC burden, 240 ms coupling interval) originating from RV apex was initiated for ≥ 4 months using a pacemaker with a unique premature pacing algorithm as previously described[1]. Four additional healthy mongrel canines were used as control. Animal studies conformed to the Guide for the Care and Use of Laboratory Animals. Experiments were approved by the McGuire VAMC Institutional Animal Care and Use Committee.

Myocyte isolation

The procedures were as described previously[2]. Briefly, left ventricular free wall was cannulated through the left circumflex coronary artery and mounted on a Langendorff apparatus. Tissue was perfused with Ca-free Tyrode's containing BSA (0.5 mg/ml) for ~ 15 minutes, followed by same solution containing collagenase type II (1 mg/mL, Worthington) and pronase E (type XIV, 0.05 mg/mL, Sigma-Aldrich) for 12–14 min till tissue was softened. Myocytes were mechanically disaggregated, filtered through nylon mesh, transferred to Kraft-Bruhe (KB) solution, and kept at room temperature for patch clamp

recording and $[Ca]_i$ experiments (in ≤ 8 hr). Myocytes were also fixed on poly-lysine coated coverslips for immunocytochemistry/confocal microscopy.

Patch clamp experiments

Action potential and whole cell currents were recorded using the patch clamp method as previously described[2]. Experiments were controlled by pClamp 10 via Digidata 1440A, using an Axopatch 200B amplifier. Pipette tip resistance was 2–3 MΩ and tip potential was zeroed before making seal. A liquid junction potential of 10 mV was corrected during data analysis. Currents were low-pass filtered at 1 kHz (Frequency Devices) and stored for off-line analysis. Data analysis was done using Clampfit, Excel, PeakFit, and SigmaStat.

Immunoblot experiments

Whole tissue lysates (WTL) were prepared as previously described[2]. Proteins were fractionated by SDS-PAGE, blotted to PVDF membranes and the levels of proteins of interest were quantified by enhanced chemiluminescence (ECL).

Immunocytochemistry, confocal microscopy, and image analysis

Myocytes were permeabilized and incubated with primary/Alexa-conjugated secondary antibody pairs. Plasma membrane was stained by Alexa-conjugated wheat germ agglutinin (WGA). Nuclei were stained with 4',6-diamidino-2-phenylindole (DAPI). Fluorescence images were obtained with a Zeiss 710 confocal microscope, and analyzed using NIH ImageJ.

Monitoring intracellular Ca

Fluo-4–loaded myocytes were placed on the stage of an epifluorescence microscope, superfused with bath solution and paced by field stimulation (CL 2 s). Fluo-4 was excited by 490/10 nm light and emission was measured at 535/50 nm.

Statistical analysis

Statistical analysis was done using SigmaStat v. 2. T-test was used to compare 2 groups (e.g. PVC vs CON), and a difference reaching $p < 0.05$ was considered significant.

On-line supplemental data

Details in experimental setups, data acquisition and analysis are provided in on-line 'Detailed Methods'. Numerical values of quantified parameters are listed in on-line 'Tables S1 – S3'.

RESULTS

On average PVC myocytes had larger values of cell capacitance than CON myocytes (225±6 vs 189±5 pF, n=50 and 51, $p < 0.001$), suggesting larger cell sizes in PVC-induced CM. PVC myocytes also exhibited significantly larger length-to-width ratios than CON myocytes (Fig. 1A), similar to cellular enlargement seen in chamber dilation. This indicates that

although there was no detectable sign of myocyte loss in PVC-induced CM[1], the myocytes did respond to the chronic stress of ventricular bigeminy by cellular hypertrophy.

Action potential configurations and durations

Fig. 1B depicts representative AP traces recorded from CON and PVC myocytes. We compared the action potential duration (Fig. 1C), and the degrees of 'beat-to-beat' variations in APDs between these two groups of myocytes (Fig.1D and 1E). The latter is believed to be a better predictor for arrhythmia risk[3].

CON myocytes had an average APD of 455±20 ms. There was a modest degree of beat-to-beat variations in APD. One example is shown in Fig. 1D, which plots APD_{n+1} against APD_n for fifty consecutive APs in a CON myocyte. The beat-to-beat variations in APD were quantified by the standard deviation of successive differences (SDSD) in APD[4]. Fig. 1E plots SDSD values of individual CON myocytes grouped by the hearts they were isolated from.

Relative to CON, PVC myocytes had prolonged APD (649±47 ms, $p < 0.01$). More importantly, some PVC myocytes exhibited extreme APD variability (one example shown in Fig. 1D). Their SDSD values were > 100 ms, not seen in the CON myocyte group (Fig. 1E). As a whole, PVC myocytes had SDSD in APD at 63.0±12.7 ms, significantly larger than that of CON myocytes (26.5±1.5 ms, $p < 0.05$).

To explore the mechanisms of APD prolongation and exaggerated beat-to-beat variations seen in PVC myocytes, we quantified the densities of key currents (patch clamp of single myocytes) and their subunit protein expression (immunoblots of tissue samples). These two analyses are complementary to each other. Patch clamp of single myocytes has limitations due to cell isolation and limited number of myocytes examined. Immunoblots of whole tissue lysates represent averaged data from multi-cellular samples. Corroboration between these two sets of data strengthens both.

Transient outward current (I_{to})

I_{to} contributes to phase 1 repolarization in cardiac myocytes. By setting the rate of phase 1 repolarization and thus the early plateau voltage, I_{to} can indirectly affect APD by influencing the activation of I_{CaL}[5]. The peak amplitude of I_{to} (quantified at +50 mV) was markedly reduced in PVC relative to CON myocytes (Fig. 2A). On the other hand, there was no difference between CON and PVC myocytes in the voltage-dependence of I_{to} inactivation or kinetics of I_{to} restitution (Fig.2B and 2C).

The major I_{to} channels in canine ventricular myocytes are composed of Kv4.3 (pore-forming) and KChIP2 (auxiliary) subunits[6, 7]. KChIP2 promotes cell surface Kv4.3 expression (thus increasing I_{to} amplitude) and modulates Kv4.3 gating kinetics (slowing the fast phase of inactivation and accelerating restitution)[8]. In both CON and PVC LV samples Kv4.3 mAb detected a 73 kDa band (expected Kv4.3 size), and KChIP2 mAb detected a 32 kDa band (expected size for KChIP2a/2b[9]) (Fig. 2D, top). Densitometry quantification showed that both Kv4.3 and KChIP2 protein levels were reduced in PVC-induced CM (Fig. 2D, bottom), although only the latter reached a p value of < 0.05. These data indicate that I_{to}

current density was reduced after chronic PVC, due to a downregulation of I_{to} channel subunits.

Inward rectifier current (I_{K1})

I_{K1} sets the resting membrane potential (RMP) and contributes to phase 3 repolarization in cardiac myocytes. Fig. 3A depicts the current-voltage relationships of I_{K1} in CON and PVC myocytes. PVC I_{K1} was reduced in both inward and outward directions. Outward I_{K1} was quantified at −70 mV and was almost 50% reduced in PVC relative to CON myocytes (1.4±0.1 vs 2.6±0.2 pA/pF, $p < 0.001$). In canine ventricular myocytes, I_{K1} channels are composed of Kir2.1 and Kir2.2 subunits[10]. Kir2.1 Ab detected a 50-kDa band (expected Kir2.1 size) in all 4 CON samples and 3 of the 4 PVC samples (Fig. 3B). In the remaining PVC sample, the Kir2.1 immunoreactive band was smaller than 50 kDa. The reason for this difference is unclear. Kir2.2 Ab detected a 50-kDa band in all CON and PVC samples. Compared to CON samples, PVC samples had the same Kir2.1 level but lower Kir2.2 level (Fig. 3B), suggesting that I_{K1} reduction in PVC myocytes was due to a downregulation of the Kir2.2 protein. Translating this finding to *in situ* heart suggests that a decrease in I_{K1} will increase the membrane resistance at diastole, making the myocytes more prone to depolarization by small inward currents, e.g. transient inward currents, thus increasing the risk for triggered arrhythmia.

L-type Ca current (I_{CaL})

I_{CaL} is the major driving force to maintain the positive plateau voltage of cardiac action potentials. I_{CaL} also provides Ca trigger to induce Ca release from SR during E-C coupling, and helps replenish the SR Ca stores[11]. Relative to CON myocytes, PVC myocytes had reduced I_{CaL} current density (3.3±0.2 vs 4.8±0.3 pA/pF, $p < 0.001$, Fig. 4A). Cav1.2 mAb detected a 240-kDa band in both CON and PVC samples (Fig. 4B, top), consistent with glycosylated Cav1.2 protein. The Cav1.2 protein level was relatively low in 1 of the 5 CON samples and in 2 of the 4 PVC samples. Although the average Cav1.2 protein level was lower in PVC than CON samples, the difference did not reach a statistically significant level. As will be shown below, the decrease in I_{CaL} current density was related to dyad remodeling in PVC-induced CM, key to the deterioration of ventricular contractility.

Rapid and slow delayed rectifier currents (I_{Kr} and I_{Ks})

It has been shown that both I_{Kr} and I_{Ks} are important contributors to action potential repolarization in canine ventricular myocytes[3, 12]. I_{Kr} and I_{Ks} overlap with I_{to} and I_{CaL} in the voltage range of activation, but are 5–10 times smaller in amplitude than I_{to} and I_{CaL} (Fig. 5A, vs Fig 2A and Fig. 4A). To separate the two delayed rectifier currents from I_{to} and I_{CaL} and from each other, we recorded I_{Kr} as tail currents at −50 mV after a 5-s depolarizing pulse to 0 mV, and I_{Ks} as tail currents at 0 mV after a 5-s depolarizing pulse to +50 mV. The rationale and validation are presented in Fig. 5B, with details of data analysis provided in on-line Detailed Methods. On average, there was no statistically significant change in I_{Kr} or I_{Ks} in PVC relative to CON myocytes (Fig. 5C). However, as will be shown below, I_{Kr} and I_{Ks} could contribute to APD variations in PVC myocytes depending on the degree of remodeling of other plateau currents.

I_{Ks} channels are composed of KCNQ1 (pore-forming) and KCNE1 (auxiliary) subunits[13], while I_{Kr} channels are composed of ERG1 (pore-forming) and KCNE2 (auxiliary) subunits[14]. Immunoblot experiments showed that the KCNQ1 and ERG1 levels were uneven among the CON and PVC samples, while the KCNE1 and KCNE2 levels were relatively homogeneous (Fig. 5C). Overall, there were no statistically significant changes in these channel subunit protein levels in PVC samples.

Excitation-contraction (E-C) coupling

Deterioration of ventricular contractile function could be due to impairment in Ca-induced Ca release secondary to the decrease in I_{CaL}. Additionally, impairment in the SR function (increase in Ca leak and/or a decrease in SR Ca pump function) could lead to a decrease in SR Ca stores. To test these possibilities, we measured fluorescence signals ($\Delta F/F_o$) from myocytes loaded with a low-affinity Ca-sensitive fluorescent dye (Fluo-4) in response to protocols designed to quantify these processes[15] (details in on-line Detailed Methods). Fig. 6A depicts exemplar time courses of such experiments carried out on a CON and a PVC myocyte. Data summary in Fig. 6B shows that while PVC myocytes suffered a significant decrease in Ca-induced Ca release from SR, they did not have more Ca leak from SR or reduced SR Ca stores.

Dyad remodeling in PVC myocytes revealed by confocal microscopy

We used confocal microscopy to monitor the immunofluorescence signals from 2 key proteins involved in E-C coupling: Cav1.2 and RyR2. We also monitored junctophilin-2 (JPH-2), a scaffolding protein believed to play a key role in stabilizing the dyad structures[16]. Fluorescently tagged wheat-germ agglutinin (WGA) served as a reference for t-tubule locations. Fig. 7A shows that in CON myocytes, Cav1.2, JPH-2, and RyR2 all manifested clear striation patterns. JPH-2, RyR2 and, to a lesser degree, Cav1.2 showed colocalization with WGA (Fig. 7B). These data reflect tight dyad organization in CON myocytes, where Cav1.2 channels in the t-tubule membrane are juxtaposed to RyR2 channels in the junctional SR membrane to afford efficient Ca-induced Ca release during E-C coupling[11].

In PVC myocytes, although JPH-2 and RyR2 maintained clear striation patterns and the same degree of colocalization with WGA as in CON myocytes, the Cav1.2 distribution pattern was clearly different: it was distributed as small puncta with occasional faint striations. There was much less colocalization between Cav1.2 and WGA in PVC myocytes.

The confocal images in Fig. 7A suggested that JPH-2 protein might be reduced in PVC myocytes. This was confirmed in immunoblot experiments, which also revealed a tight correlation between JPH-2 and Cav1.2 in the degree of their reduction among PVC samples (Fig. 7C). PVC myocytes had more abundant and larger vesicles positive for LAMP1, a lysosome marker (Fig.7D and 7E). Importantly, most of the $LAMP1^+$ vesicles in PVC myocytes were also positive for JPH-2, suggesting an increase in lysosomal degradation of JPH-2 in PVC hearts.

DISCUSSION

In this study we report four major findings in a canine model of premature ventricular contraction-induced cardiomyopathy. First, there was a reduction in I_{to} and I_{K1} current densities, along with a prolongation of average APD in PVC ventricular myocytes. Second, PVC myocytes manifested exaggerated beat-to-beat variations in APD. The temporal heterogeneity in APD could be an important substrate for reentrant ventricular arrhythmia. Third, Cav1.2 protein expression and I_{CaL} current density were reduced in PVC-induced CM. Fourth, Cav1.2 protein was relocated away from the t-tubules in PVC myocytes. The latter two findings could explain impairment of E-C coupling and contractile dysfunction in PVC-induced CM.

Molecular mechanisms for exaggerated beat-to-beat variations in APD of electrically remodeled PVC myocytes

PVC myocytes manifested exaggerated beat-to-beat variations in APD, to a level (> 100 ms in standard deviations of successive differences in APD) not seen in CON myocytes. To explore the mechanism(s), and in view of the recent suggestions of stochastic nature of action potential determinants[3], we analyzed the relationship between APD and individual currents among myocytes. This was done by two methods: linear regression and Pearson correlation coefficient. Fig.8A and 8B show that these two sets of analysis produce consistent results: negative slopes in linear regression are associated with negative correlation coefficients, positive slopes in linear regression associated with positive correlation coefficients, and flat linear regression associated with ~ zero correlation coefficient.

In CON myocytes, I_{CaL} and APD were unrelated, while I_{to}, I_{K1} and I_{Kr} were negatively related to APD (decrease in current linked to APD prolongation). These are consistent with computer model simulations of canine ventricular action potentials[3], and support the role of these 3 outward currents in AP repolarization. However, I_{Ks} was positively related to APD (decrease in I_{Ks} linked to APD shortening). This is possible if I_{Ks} was small under the basal conditions, making little or no contribution to AP repolarization at a cycle length of 1 s.

In PVC myocytes, I_{K1} and I_{Kr} were negatively related to APD, supporting the role of these 2 currents in AP repolarization in electrically remodeled PVC myocytes. Surprisingly, I_{CaL} became negatively related to APD while I_{to} positively related to APD, i.e. reducing I_{CaL} or increasing I_{to} was linked to APD prolongation. This can be explained by the interplay between I_{to} and I_{CaL} during the early plateau phase[5]: a modest increase in I_{to} in conjunction with a modest decrease in I_{CaL} could create a marked ‘spike-and-dome’ morphology, and the delay in secondary I_{CaL} activation, the ‘dome’, caused APD prolongation. The PVC #2 myocyte shown in Fig.8C and 8D supports this scenario. Its I_{to} was relatively strong but I_{CaL} was greatly attenuated. We speculate that APs fluctuated between a ‘spike-and-dome’ morphology with long APDs due to the prominent delay in the rising phase of plateau, and the ‘loss-of-dome’ morphology with very short APDs due to the loss of plateau phase.

In PVC myocytes, I_{Ks} became negatively related to APD, supporting a scenario that under stressful conditions, I_{Ks} as a ‘repolarization reserve’ may become more important in APD

repolarization[17]. The PVC #3 myocyte in Fig.8C and 8D supports this scenario. It had short APDs and even less beat-to-beat variations than seen in CON myocytes. It had reduced I_{to}, I_{K1} and I_{CaL}, but its I_{Ks} (as well as I_{Kr}) was relatively large. We speculate that the delayed rectifier currents tightly regulated the APD to keep it within a narrow range. This is consistent with computer model simulations[3]: β-adrenergic stimulation increases I_{Ks} and reduces beat-to-beat variations in repolarization of canine ventricular myocytes.

Impairment of E-C coupling in PVC heart – more about Cav1.2 than RyR2

Our data suggested two defects in E-C coupling in PVC-induced CM. First, the Cav1.2 protein expression and I_{CaL} density were reduced. Second, Cav1.2 protein was relocated away from the t-tubules. This observation is similar to the 'orphaned RyR2' seen in myocytes from failing hearts of spontaneously hypertensive rate (SHR-HF[18]). In SHR-HF myocytes, RyR2s are orphaned by the moving-away of t-tubules. However, in PVC myocytes RyR2s maintained close connection with z-lines and were orphaned by the moving-away of Cav1.2 channels. In either case, the orphaned RyR2s would have reduced efficiency in Ca release as observed experimentally[18] (Fig. 6).

Limitations

(1) While this manuscript does not address all possible mechanisms related to risk of arrhythmias and contractile impairment associated to PVCs, we present a complete body of data that provides mechanistic insights into these issues. *(2)* The presented findings were performed only on the LV free wall. Other regions of the heart unexamined in the present study may be also affected by chronic PVCs and contribute to the susceptibility to arrhythmias. These limitations provides the grounds for future experiments to explore several detailed pathways,

CONCLUSIONS

Chronic frequent PVCs induce electrical remodeling characterized by increase in APD dispersion and decreased densities of both outward (I_{to} and I_{K1}) and inward (I_{CaL}) currents. The exaggerated beat-to-beat variations in APD may pose an elevated risk for reentrant ventricular arrhythmia. The downregulation of Cav1.2 and loss of Cav1.2 registry with RyR2 could explain the contractile dysfunction in PVC-induced cardiomyopathy.

Supplementary Material

Refer to Web version on PubMed Central for supplementary material.

Acknowledgments

We thank Drs. Kenneth A. Ellenbogen and Clive Baumgarten for their assistance and discussion during this study. Microscopy was performed at the Virginia Commonwealth University – Department of Neurobiology & Anatomy Microscopy Facility, supported in part by NIH-NINDS Center Core Grant 5P30NS047463.

Funding: This study was supported by American Heart Association/National Center Scientist Development Grant (to JFH, Grant ID # 12SDG9310032), and by RO1 from National Heart, Blood and Lung Institute of National Institutes of Health (to GNT, HL107294).

Disclosure: Research Grants from St. Jude Medical, Inc and Boston Scientific, Corp (to JFH).

Abbreviations

PVC	premature ventricular contraction
E-C coupling	excitation-contraction coupling

REFERENCES

1. Huizar JF, Kaszala K, Potfay J, et al. Left ventricular systolic dysfunction induced by ventricular ectopy. A novel model for premature ventricular contraction-induced cardiomyopathy. Circ Arrhythm Electrophysiol. 2011; 4:543–549. [PubMed: 21576277]
2. Liu X-S, Jiang M, Zhang M, Tang D, Higgins RSD, Tseng G-N. Electrical remodeling in a canine model of ischemic cardiomyopathy. Am J Physiol. 2007; 292:H560–H571.
3. Heijman J, Zaza A, Johnson DM, Rudy Y, Peeters RLM, Volders PGA, Westra RL. Determinants of beat-to-beat variability of repolarization duration in the canine ventricular myocyte: a computational analysis. PLoS-One. 2013; 9:e1003202.
4. Brennan M, Palaniswami M, Kamen P. Do existing measures of Poincare plot geometry reflect nonlinear features of heart rate variability? IEEE Transactions on Biomedical Engineering. 2001; 48:1342–1347. [PubMed: 11686633]
5. Greenstein JL, Wu R, Po S, Tomaselli GF, Winslow RL. Role of the calcium-independent transient outward current I_{to1} in shaping action potential morphology and duration. Circ Res. 2000; 87:1026–1033. [PubMed: 11090548]
6. Dixon JE, Shi W, Wang H-S, McDonald C, Yu H, Wymore RS, Cohen IS, McKinnon D. Role of the Kv4.3 K^+ channel in ventricular muscle. A molecular correlate for the transient outward current. Circ Res. 1996; 79:659–668. [PubMed: 8831489]
7. Rosati B, Pan Z, Lypen S, Wang H-S, Cohen IS, Dixon JE, McKinnon D. Regulation of *KChIP2* potassium channel β subunit gene expression underlies the gradient of transient outward current in canine and human ventricle. J Physiol. 2001; 533:119–125. [PubMed: 11351020]
8. An WF, Rowlby MR, Betty M, Cao J, Ling H-P, Mendoza G, Hinson JW, Mattsson KI, Strassle BW, Trimmer JS, Rhodes KJ. Modulation of A-type potassium channels by a family of calcium sensors. Nature. 2000; 403:553–556. [PubMed: 10676964]
9. Decher N, Barth A, Gonzalez T, Steinmayer K, Sanguinetti MC. Novel KChIP2 isoforms increase functional diversity of transient outward potassium currents. J Physiol. 2004; 557.3:761–772. [PubMed: 15107477]
10. Houtman MJC, Takanari H, Kok BGJM, van Eck M, Montagne DR, Vos MA, de Boer TP, van der Heyden MAG. Experimental mapping of the canine KCNJ2 and KCNJ12 gene structures and functional analysis of the canine $K_{IR}2.2$ ion channel. Frontiers in Physiology. 2012
11. Bers DM. Cardiac excitation-contraction coupling. Nature. 2002; 415:198–205. [PubMed: 11805843]
12. Jost N, Virag L, Comtois P, et al. Ionic mechanisms limiting cardiac repolarization reserve in humans compared to dogs. Journal of Physiology. 2013; 591:4189–4206. [PubMed: 23878377]
13. Sanguinetti MC, Curran ME, Zou A, Shen J, Spector PS, Atkinson DL, Keating MT. Coassembly of KvLQT1 and minK (IsK) proteins to form cardiac I_{Ks} potassium channel. Nature. 1996; 384:80–83. [PubMed: 8900283]
14. Jiang M, Zhang M, Tang DG, Clemo HF, Liu J, Holwitt D, Kasirajan V, Higgins RS, Wettwer E, Tseng G-N. KCNE2 protein is expressed in ventricles of different species and changes in its expression contribute to electrical remodeling in diseased hearts. Circulation. 2004; 109:1783–1788. [PubMed: 15066947]
15. Shannon TR, Pogwizd SM, Bers DM. Elevated sarcoplasmic reticulum Ca^{2+} leak in intact ventricular myocytes from rabbits in heart failure. Circ Res. 2003; 93:592–594. [PubMed: 12946948]
16. Guo A, Zhang C, Wei S, Chen B, Song L-S. Emerging mechanisms of t-tubule remodeling in heart failure. Cardiov Res. 2013; 98:204–215.

17. Wang Y-H, Zankov DP, Jiang M, Zhang M, Henderson SC, Tseng G-N. $[Ca]_i$ elevation and oxidative stress induce KCNQ1 translocation from cytosol to cell surface and increase I_{Ks} in cardiac myocytes. J Biol Chem. 2013; 288:35358–35371. [PubMed: 24142691]

18. Song L-S, Sobie EA, McCulle S, Lederer WJ, Balke W, Cheng H. Orphaned ryanodine receptors in the failing heart. PNAS. 2006; 103:4305–4310. [PubMed: 16537526]

CLINICAL PERSPECTIVES

Frequent premature ventricular contractions (PVCs) is a common clinical problem, which predisposes to cardiomyopathy (CM) and increases the risk of ventricular arrhythmias and sudden cardiac death. However, the mechanisms remain poorly understood. Understanding these mechanism(s) is critical to develop therapies aimed at decreasing the morbidity and mortality related to PVCs. The present study demonstrates that in PVC-induced CM, there is prolongation and marked beat-to-beat variation of action potential duration (APD), as well as decreased outward (I_{to} and I_{K1}) and inward (I_{CaL}) currents. These changes result in increased repolarization heterogeneity and may predispose to the formation of triggered activity and malignant ventricular arrhythmias. Secondly, altered Ca-induced Ca release from SR due to decrease in I_{CaL} and Cav1.2 along with misalignment of Cav1.2 with Ryanodine receptor could explain the contractile dysfunction observed in PVC-induced CM. Future studies are needed to elucidate the subcellular and molecular mechanisms involved in these observed changes to excitation-contraction coupling and pro-arrhythmia, including alterations in gene transcription, microRNA repression, protein targeting, internalization and degradation, derangements in autonomic tone, post-extrasystolic potentiation, heart rate irregularity and abnormal LV mechanics.

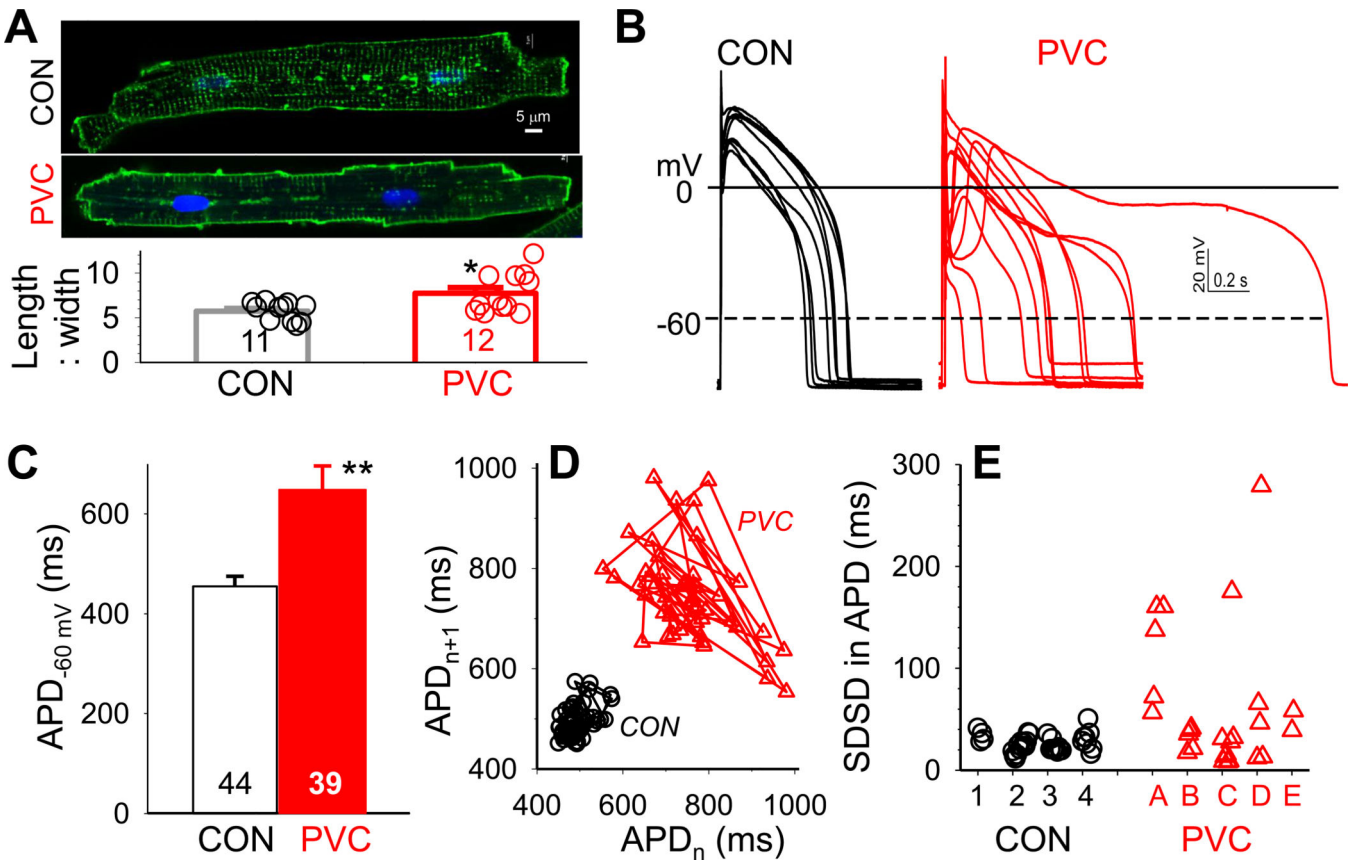

Fig. 1. PVC myocytes had prolonged action potential durations (APD) with exaggerated beat-tobeat variations

(A) Top: Images of CON and PVC myocytes with cell membrane/t-tubules stained by fluorescent WGA or di-8-ANEPPS. Bottom: Length:width ratios of CON and PVC myocytes. Data from individual myocytes shown as open circles; values of Mean±SE shown as histogram bars. **(B)** Superimposed AP traces recorded from ten CON and ten PVC myocytes. The cycle length (CL) was 1 s, except the PVC myocyte with markedly prolonged APD (CL = 2 s). **(C)** APDs quantified as time between upstroke and when membrane repolarized to −60 mV ($APD_{-60\ mV}$). **(D)** APD_{n+1} plotted against APD_n for fifty consecutive action potentials recorded from a CON and a PVC myocyte (corresponding to data points marked by solid symbols in 'D'). **(E)** Standard deviations of successive differences (SDSD) in APD. Data points from individual myocytes are grouped by the hearts they were isolated from (CON hearts 1–4, PVC hearts A–E). For this and the following figures, details of voltage-clamp protocols and data analysis are provided in on-line Detailed Methods. Numerical data values are listed in Tables S1–S3. Numbers of myocytes or samples analyzed are listed in histogram bars or insets. CON and PVC myocytes were isolated from 4 and 5 animals, respectively.

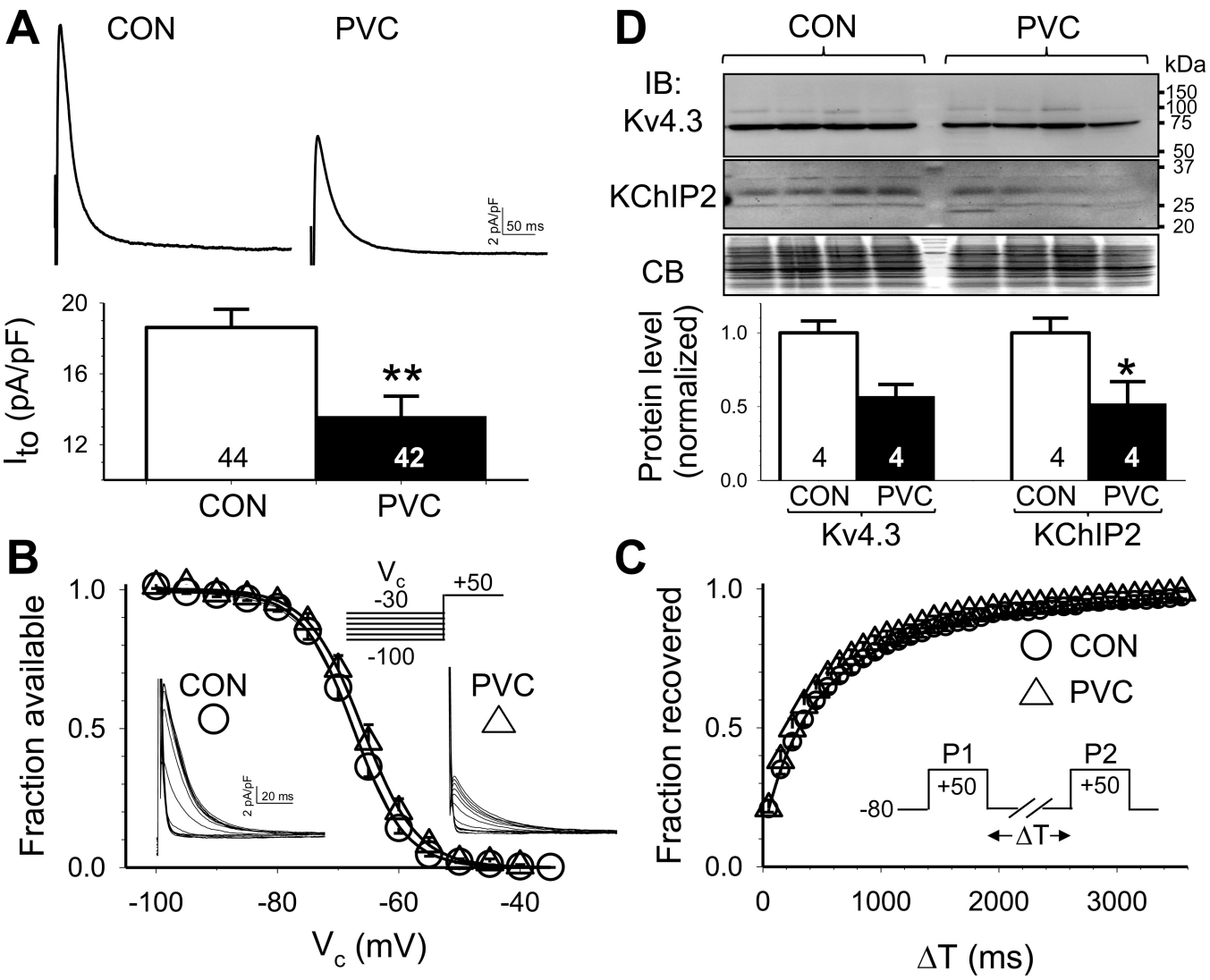

Fig. 2. PVC myocytes had reduced transient outward (I_{to}) current density but unaltered I_{to} gating kinetics, accompanied by a downregulation of I_{to} channel subunits

(A) *Top*: Representative I_{to} traces recorded from CON and PVC myocytes. *Bottom*: peak I_{to} densities in CON and PVC myocytes. **(B)** Voltage-dependence of I_{to} inactivation. **(C)** Time course of recovery from inactivation (I_{to} restitution). **(D)** Immunoblot quantification of protein levels of pore-forming and auxiliary subunits of I_{to} channels (Kv4.3 and KChIP2). *Top*: Images of immunoblots and Coomassie blue stain of the gel (CB, as loading control). Size marker bands (in kDa) are shown on the right. *Bottom*: Densitometry quantification of Kv4.3 and KChIP2 protein levels.

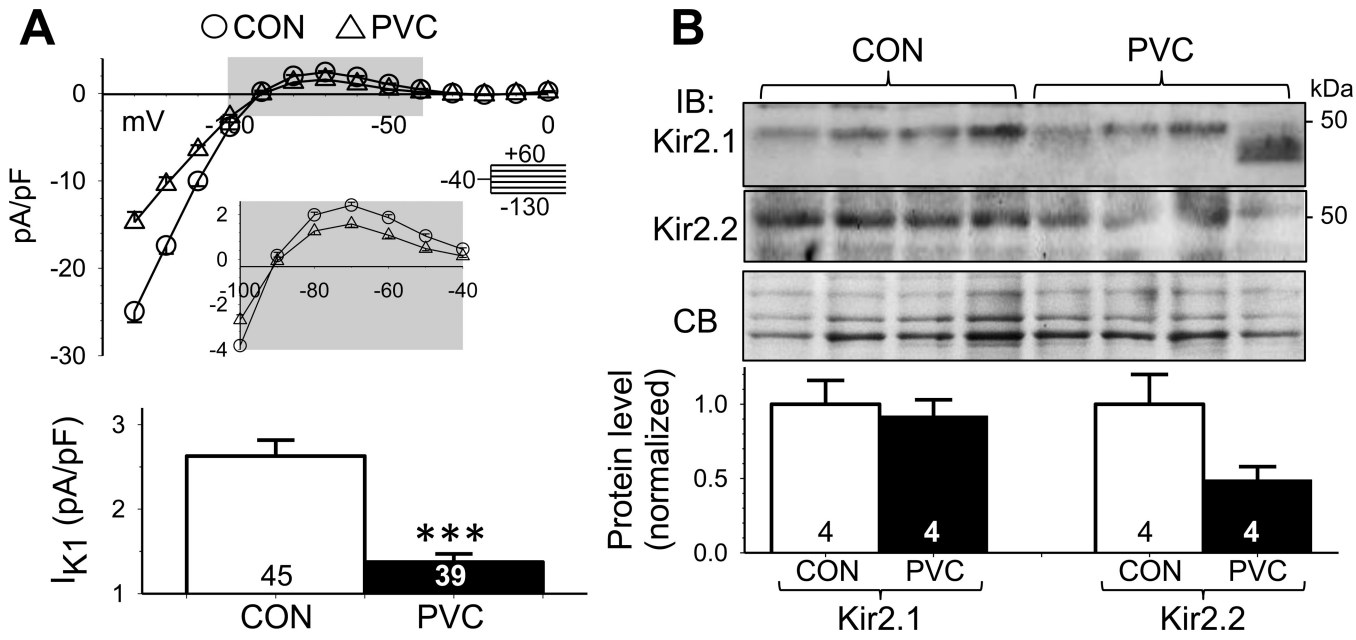

Fig. 3. PVC myocytes had reduced inward rectifier (I_{K1}) current densities, accompanied by a downregulation of Kir2.2

(A) *Top*: Average steady-state current-voltage (I-V) relationships of CON and PVC myocytes. The enlarged view of gray shading area highlights the outward portion of I_{K1}. *Bottom*: outward I_{K1} densities at −70 mV in CON and PVC myocytes. **(B)** Immunoblot quantification of I_{K1} channel subunits, Kir2.1 and Kir2.2, in LV samples. Data analysis and presentation are the same as Fig. 2D.

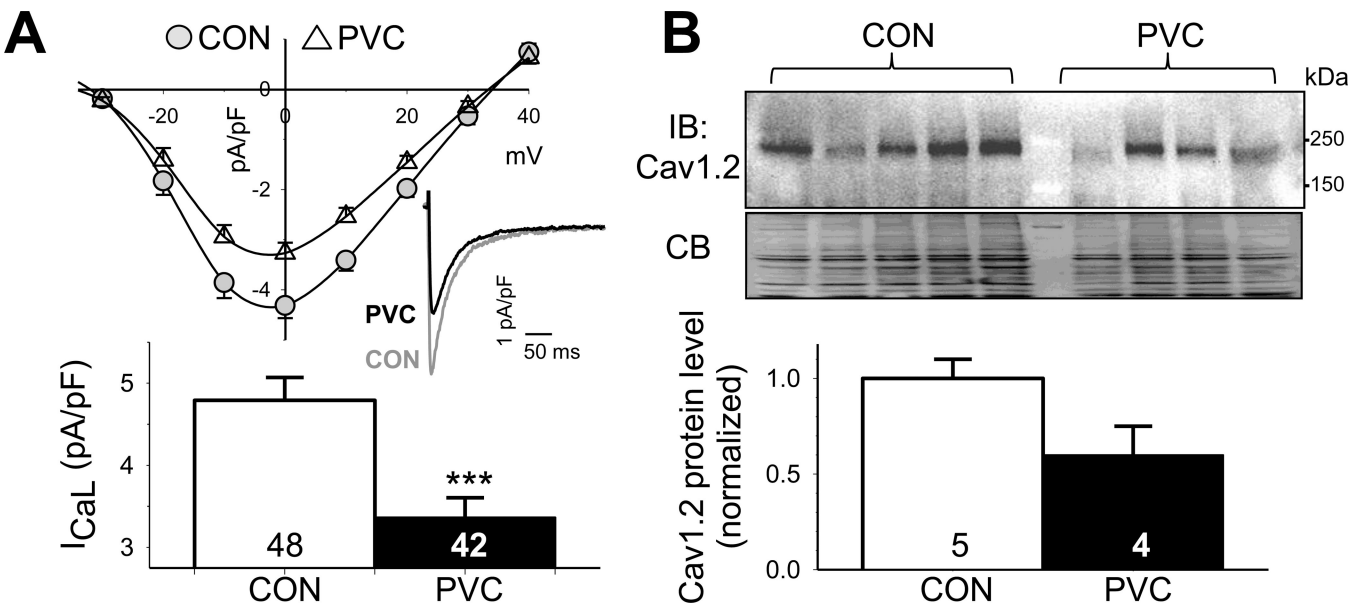

Fig. 4. PVC myocytes had reduced peak L-type Ca (I_{CaL}) current density, accompanied by a downregulation of pore-forming subunit (Cav1.2)

(A) *Top*: I–V of I_{CaL}, with representative I_{CaL} traces recorded at 0 mV from CON and PVC myocytes shown (*inset*). Bottom: peak I_{CaL} densities at 0 mV in CON and PVC myocytes. **(B)** Immunoblot quantification of Cav1.2. Data analysis and presentation are the same as Fig. 2D.

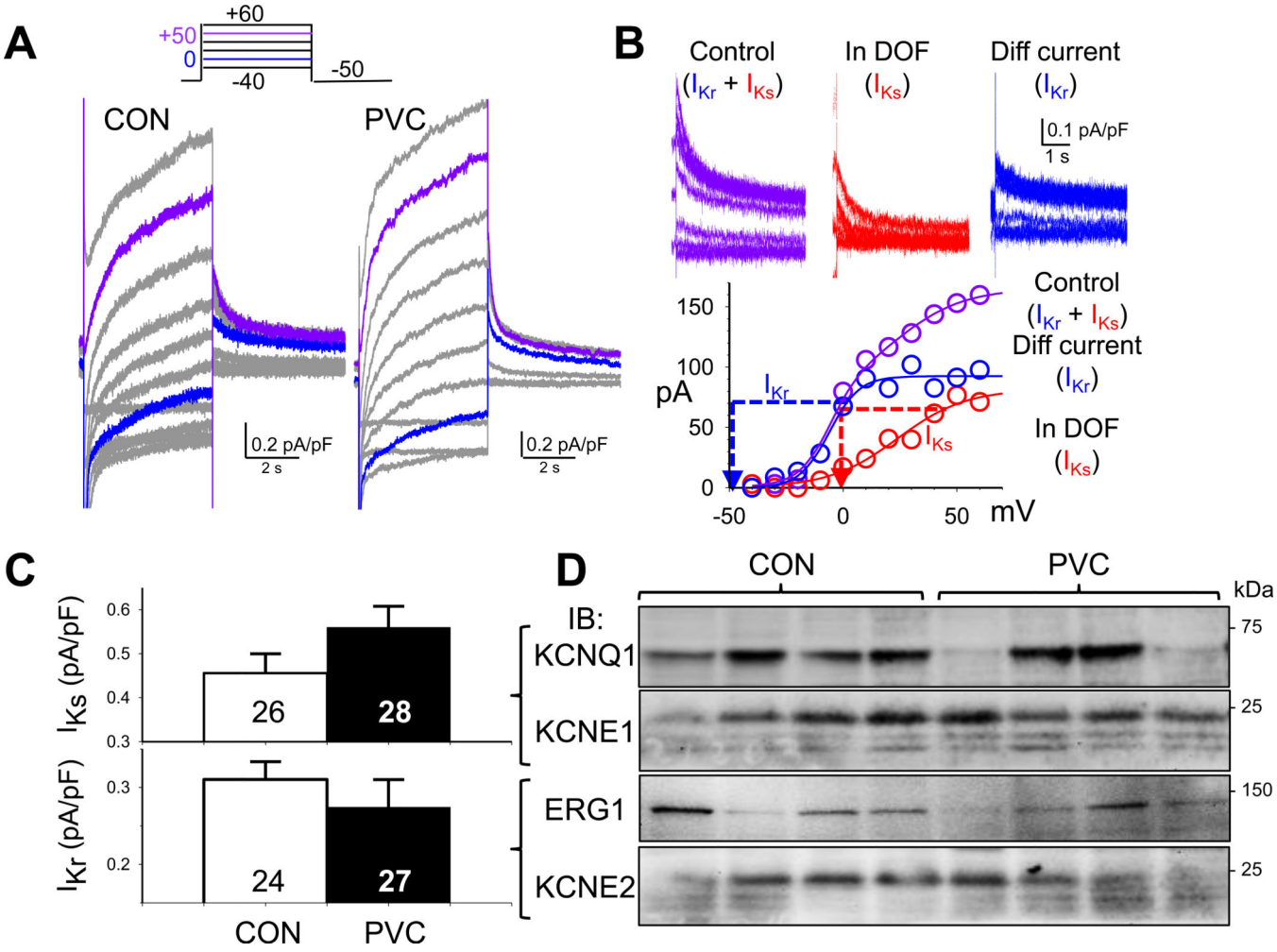

Fig. 5. No consistent or statistically significant differences in rapid and slow delayed rectifier currents (I_{Kr} and I_{Ks}) between PVC and CON myocytes

(A) Combined 'I_{Kr}+I_{Ks}' traces in a CON and a PVC myocyte, elicited by the diagrammed voltage clamp protocol. **(B)** Validation of I_{Kr} and I_{Ks} quantification. The rationale, experimental protocols and data analysis are provided in on-line Detailed Methods. **(C)** Comparison of I_{Ks} and I_{Kr} tail current densities between CON and PVC myocytes. **(D)** Immunoblot quantification of pore-forming and auxiliary subunits of I_{Ks} (KCNQ1 and KCNE1) and I_{Kr} (ERG1 and KCNE2). Densitometry quantification as described for Fig. 2D.

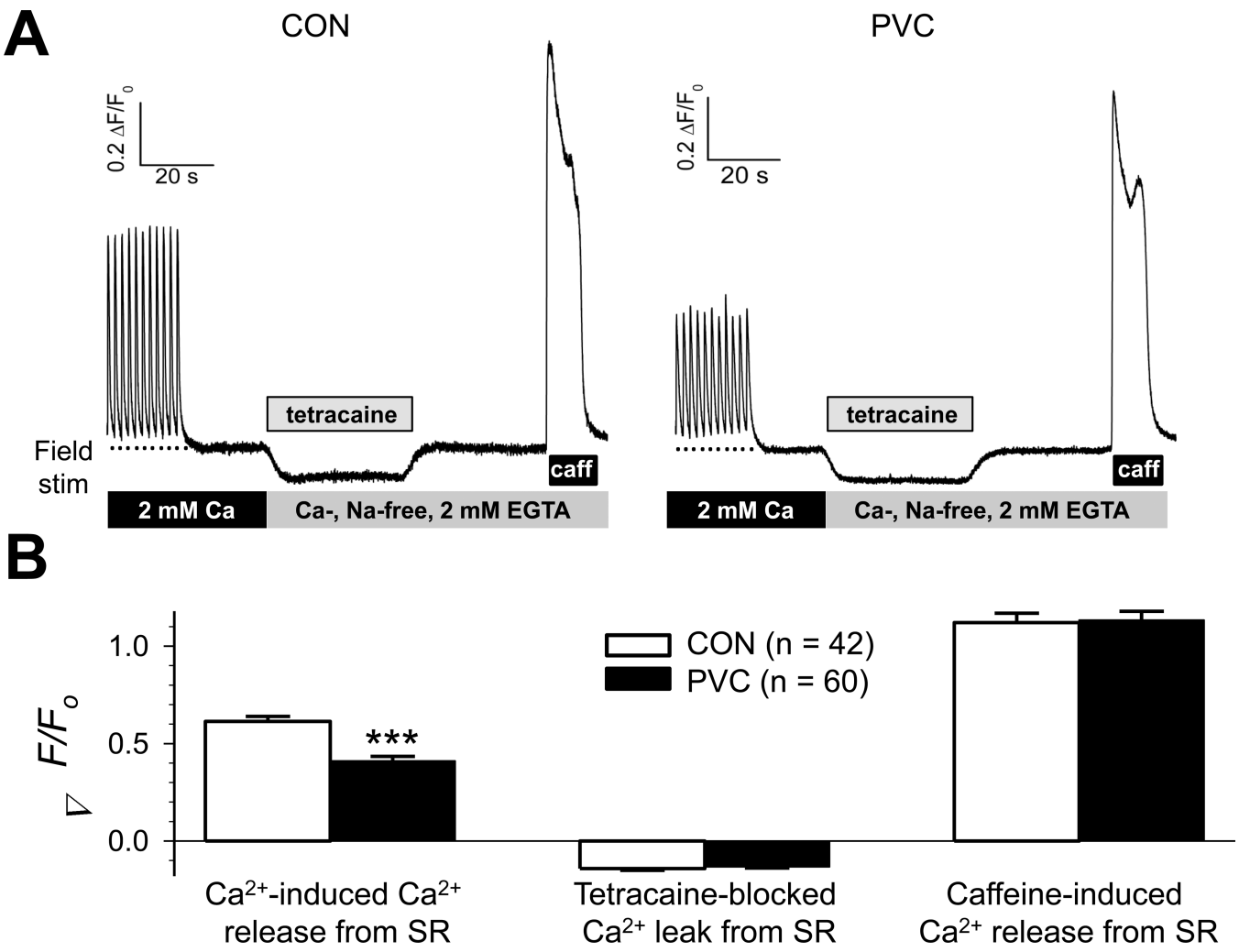

Fig. 6. PVC myocytes had reduced amplitudes of Ca-induced Ca release from SR, but no significant change in either SR Ca leak or SR Ca store

(A) Representative fluorescence signals from fluo-4-loaded CON and PVC myocytes. **(B)** Data summary for CON and PVC myocytes. Details of experimental protocols and data analysis are provided in on-line Detailed Methods.

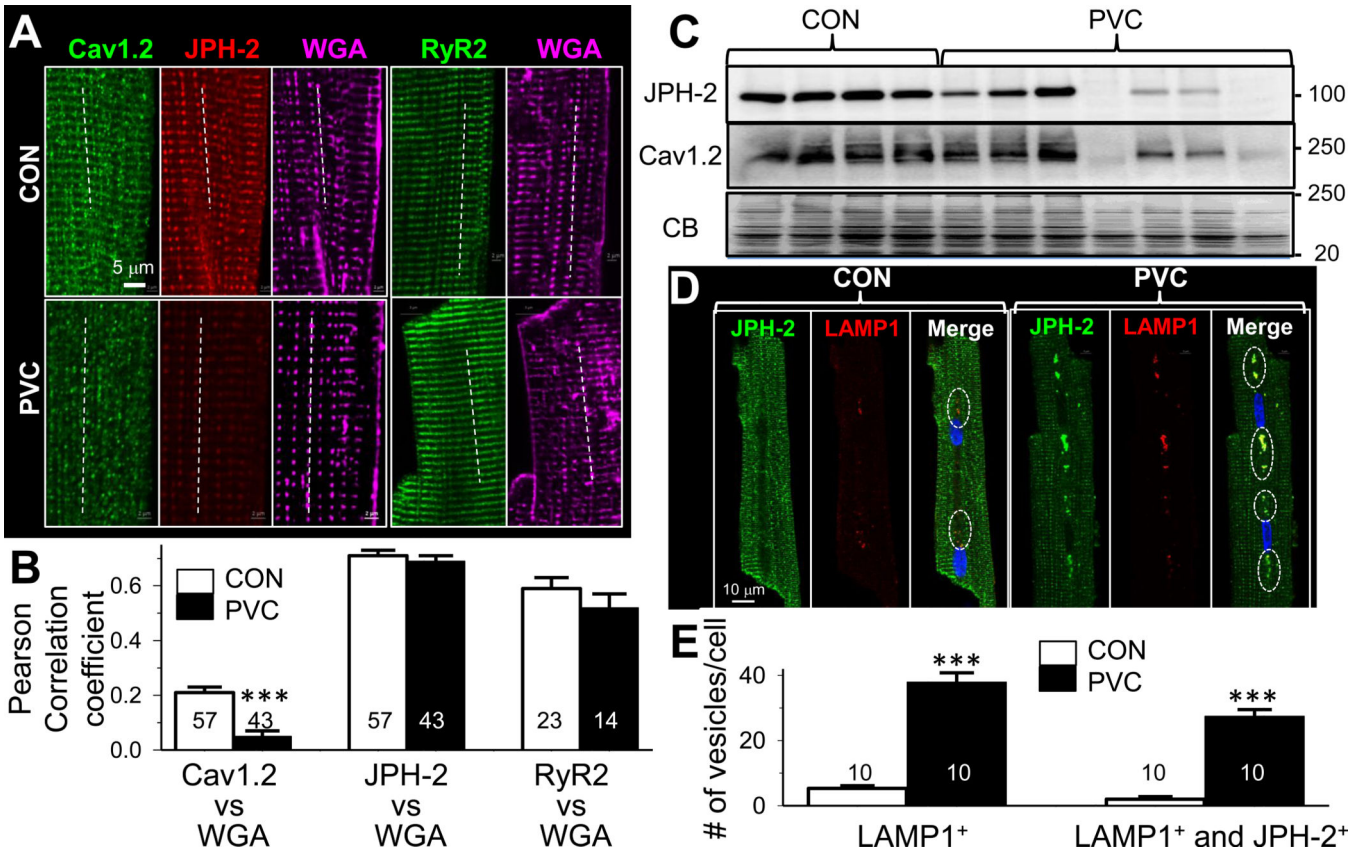

Fig. 7. PVC myocytes showed dyad remodeling with disarray in Cav1.2 distribution

(A) Confocal images of Cav1.2, junctophilin-2 (JPH-2) immunofluorescence signals from the same myocytes, and RyR2 from 2 other myocytes. Alexa647-WGA signals served as a reference for t-tubule locations. Dotted lines depict how colocalization between WGA and Cav1.2, JPH-2 or RyR2 was analyzed (more in *on-line*Detailed Methods). **(B)** Summary of Pearson correlation coefficients between WGA and Cav1.2 (left), JPH-2 (middle) or RyR2 (right) in CON and PVC myocytes (*** $p < 0.001$). **(C)** JPH-2 and Cav1.2 immunoblots of the same set of CON and PVC hearts. **(D)** JPH-2 and LAMP1 signals in a CON and a PVC myocytes. Open circles in the 'Merge' panel highlight JPH-2/LAMP1 colocalization. **(E)** Quantification of vesicles per cell that are positive for LAMP1 ($LAMP1^+$) or both $LAMP1^+$ and $JPH\text{-}2^+$.

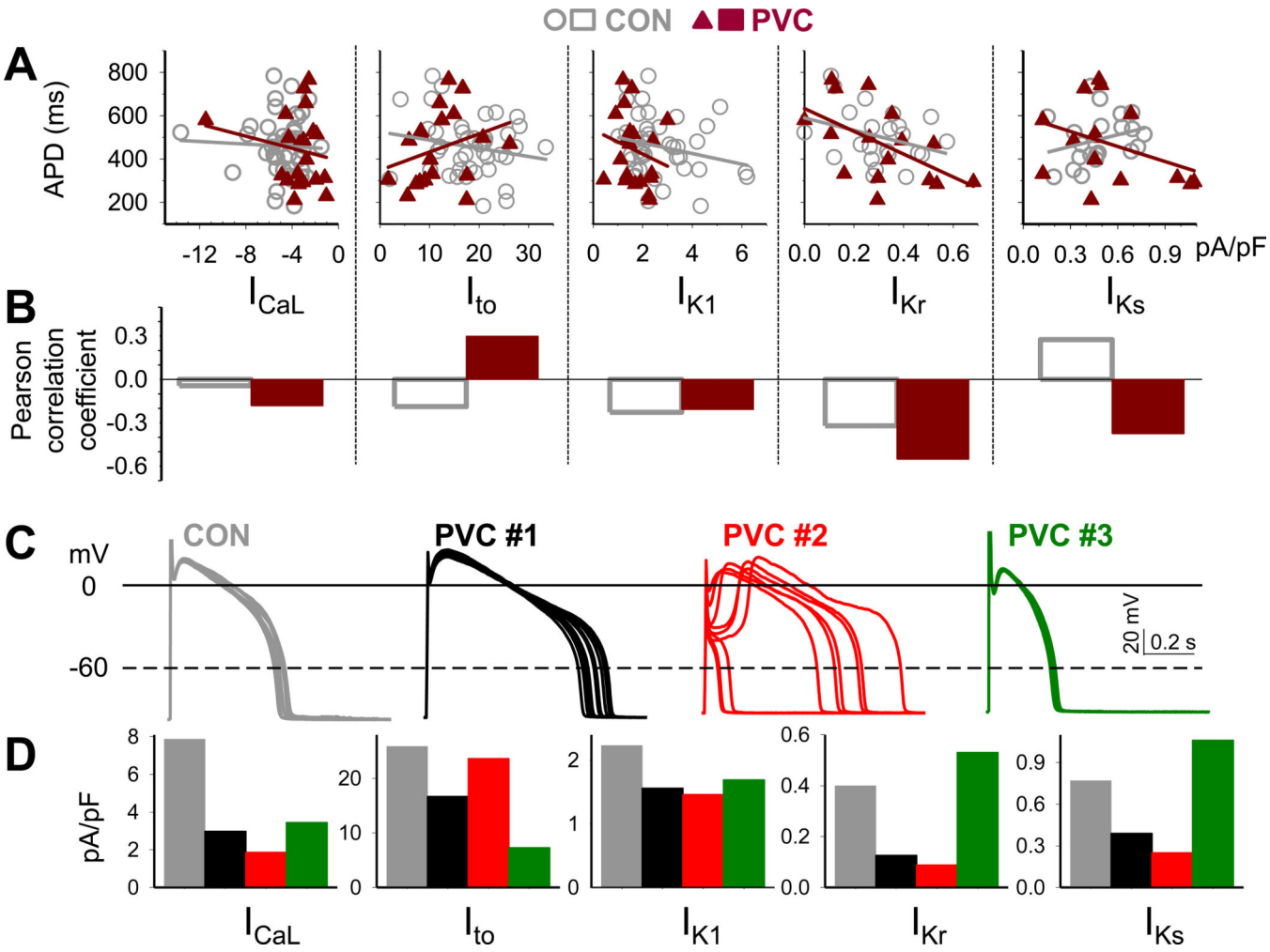

Fig. 8. Correlation between action potential duration (APD), beat-to-beat variability of APD, and current densities of I_{CaL}, I_{to}, I_{K1}, I_{Kr} and I_{Ks} of individual CON and PVC myocytes

(A) Linear regression between APDs (quantified as described for Fig. 1) and current densities (quantified as described for Fig. 2 – 5). **(B)** Pearson correlation coefficient between APDs and current densities. **(C)** Exemplar action potentials of CON and PVC myocytes and **(D)** corresponding I_{CaL}, I_{to}, I_{K1}, I_{Kr} and I_{Ks} current densities, color-coded as dark gray (CON), black (PVC #1), red (PVC #2) and dark green (PVC #3).